Novel heterozygous mutation c.4282G>T in the *SCN5A* gene in a family with Brugada syndrome

JIAN-FANG ZHU[1*], LI-LI DU[2*], YUAN TIAN[3*], YI-MEI DU[2], LING ZHANG[2], TAO ZHOU[4] and LI TIAN[5]

[1]Central Laboratory; [2]Ion Channelopathy Research Center, Institute of Cardiology;
Departments of [3]Geriatrics and Nursing, [4]Otolaryngology and [5]Pediatrics, Union Hospital,
Tongji Medical College, Huazhong University of Science and Technology, Wuhan, Hubei 430022, P.R. China

Received February 26, 2014; Accepted August 20, 2014

DOI: 10.3892/etm.2015.2361

Abstract. Brugada syndrome (BrS) is a rare, inherited arrhythmia syndrome. The most well-known gene that is responsible for causing BrS is *SCN5A*, which encodes the human cardiac Na^+ channel ($Na_v1.5$) α subunit. To date, it has been reported that >100 mutations in *SCN5A* can cause BrS. In the present study, a novel BrS-associated $Na_v1.5$ mutation, A1428S, was identified in a proband who was successfully resuscitated from an episode of sudden collapse during walking. This mutation was further confirmed by polymerase chain reaction (PCR)-restriction fragment length polymorphism analysis, which showed that the PCR fragment containing the mutation A1428S could be cut by the restriction enzyme *Nsi*1, yielding two shorter DNA fragments of 329 and 159 bp, which were not present in family members homozygous for the wild-type (WT) allele. Furthermore, the electrophysiological properties were analyzed by patch clamp technique. Current density was decreased in the A1428S mutant compared that in the WT. However, neither the steady-state activation or inactivation, nor the recovery from inactivation exhibited changes between the A1428S mutant and the WT. In conclusion, the results of this study are consistent with the hypothesis that a reduction in $Na_v1.5$ channel function is involved in the pathogenesis of BrS. The structural-functional study of the $Na_v1.5$ channel enhances the present understanding the pathophysiological function of the channel.

Correspondence to: Dr Li Tian, Department of Pediatrics, Union Hospital, Tongji Medical College, Huazhong University of Science and Technology, 1277 Jiefang Avenue, Wuhan, Hubei 430022, P.R. China
E-mail: doctortianli@-yahoo.com.cn

Dr Tao Zhou, Department of Otolaryngology, Union Hospital, Tongji Medical College, Huazhong University of Science and Technology, 1277 Jiefang Avenue, Wuhan, Hubei 430022, P.R. China
E-mail: entzt2013@sina.cn

*Contributed equally

Abbreviations: BrS, Brugada syndrome; ECG, electrocardiography; HEK293T cells, human embryonic kidney 293 cells; MT, mutation type; $Na_v1.5$, cardiac Na^+ channel; PCR-RFLP, polymerase chain reaction-restriction fragment length polymorphism; SCD, sudden cardiac death; WT, wild-type

Key words: Brugada syndrome, *SCN5A*, heterozygous mutation

Introduction

Brugada syndrome (BrS) is a rare, inheritable arrhythmia syndrome, which is characterized by a coved-type ST-segment elevation in the right precordial leads (V1 to V3) on surface electrocardiography (ECG) and a high incidence of sudden mortality in patients without evident structural heart disease, electrolyte disturbances or ischemia (1). The condition is considered to be responsible for 4-12% of all sudden cardiac deaths (SCDs) and 20% of SCDs in patients with the absence of structural heart disease secondary to re-entrant polymorphic ventricular tachycardia and ventricular fibrillation (2-4). The syndrome manifests primarily during adulthood, with a mean age of SCD of ~40 years (4). The diagnosis of BrS is based on the presence of coved-type ST-segment elevations in the right precordial leads (V1 to V3) on surface electrocardiography (ECG), which are characteristic of BrS type 1 ECGs, whereas saddle-back ST-segment elevations correspond to BrS type 2 and 3 ECGs (5). To confirm the diagnosis, the diagnostic ECGs should be reinforced with either personal symptoms, family history of premature SCD or at least one additional relative with a positive type 1 BrS ECG (6).

Since it was first reported by Chen *et al* in 1998 (7) that loss-of-function mutations of *SCN5A* account for the most well-known genetic substrate for BrS, mutations in 11 other genes that cause BrS have been reported. These genes include the cardiac L-type calcium channel subunits encoded by *CACNA1C* (8), *CACNB2B* (8) and *CACNA2D1* (9), sodium channel subunits encoded by *GPD1L* (9), *SCN1B* (10), *SCN1Bb* (11), *SCN3B* (12) and *MOG1* (13), transient outward potassium channel subunits encoded by *KCNE3* (14) and *KCND3* (15), the ATP-sensitive potassium channel encoded by *KCNJ8* (16) and the HCN4 channel encoded by *HCN4* (17). However, *SCN5A* remains the most frequently reported gene causing BrS to date, accounting for 15-30% of the clinically diagnosed cases (18-20).

In the present study, a novel heterozygous mutation, A1428S, was identified in the *SCN5A* gene in a patient with

BrS. The aim of the study was to characterize the biophysical properties of this novel mutation, in order to expand the spectrum of mutations causing BrS and provide evidence for the hypothesis that the loss of function of the mutant Na^+ channel ($Na_v1.5$) was involved in the pathogenesis of BrS.

Materials and methods

Patients. The study participants were identified and enrolled at Huazhong University of Science and Technology Union Hospital (Wuhan, China). Informed consent was obtained from the participants in accordance with the study protocols approved by the Ethics Committee of Huazhong University of Science and Technology. Twenty-eight family members, including 14 males and 14 females were involved in this study (Fig. 1). Detailed records on their medical history, physical examinations and 12-lead ECGs were obtained. The diagnosis of BrS was made on the basis of symptoms, physical signs and a typical ECG. Among all the family members, four members exhibited the clinical criteria of a BrS phenotype.

Direct DNA sequencing analyses. As described previously (21,22), venous blood (5 ml) was collected from the participants, and total human genomic DNA was purified with the DNA Isolation kit for Mammalian Blood (Roche Diagnostics, Indianapolis, IN, USA). Considering that *SCN5A* thus far remains the most frequently reported gene causing BrS, mutation screening of the *SCN5A* gene was carried out directly without performing linkage analysis. The entire coding exons of the *SCN5A* gene of the proband were amplified by polymerase chain reaction (PCR). Primers were designed with intronic flanking sequences according to the gene sequence described by Wang *et al* (23). Each amplicon was designed for an optimal size, with the exon centered within the amplicon. As a result, a total of 28 amplicons were used to sequence the coding region of the gene. Briefly, the PCR amplification was performed in the PTC-200 thermal cycler (MJ Research Inc., Waterdown, MA, USA) in a 25-μl reaction mixture containing 1.5 mM $MgCl_2$, 0.2 mM of each deoxyribonucleotide triphosphate (Qiagen, Hilden, Germany), 0.5 μM primers, 1 unit Taq DNA polymerase (Qiagen), and 50 ng genomic DNA. PCR was performed as follows: Initial denaturation for 5 min at 94˚C, followed by nine cycles of 45 sec at 94˚C, 45 sec at 61.5˚C and 45 sec at 72˚C, followed by 29 cycles of 45 sec at 94˚C, 45 sec at 55˚C and 45 sec at 72˚C with a separate annealing temperature at 55˚C. Direct bidirectional resequencing of all PCR-amplified products was performed with the BigDye Terminator Cycle Sequencing v3.1 kit (Applied Biosystems, Foster City, CA, USA) and electrophoresed on an ABI PRISM 3730 Genetic Analyzer (Applied Biosystems). Sequencing results from the subjects and *SCN5A* gene consensus sequences from GenBank (GenBank accession no. NM_198056; http://www.ncbi.nlm.nih.gov/genbank/) were compared using Basic Local Alignment Search Tool analysis. Mutation description was followed by the nomenclature recommended by the Human Genomic Variation Society (Carlton South, Australia). Resequencing of the mutated exon 24 of the *SCN5A* gene was performed on the other family members and 100 unrelated controls. The primers used were as follows: Forward, TGGGGTGGCTTGCTTTTCATAA; reverse, TGGGGTGCTGGACAAAGAAGAA. The evolutionary

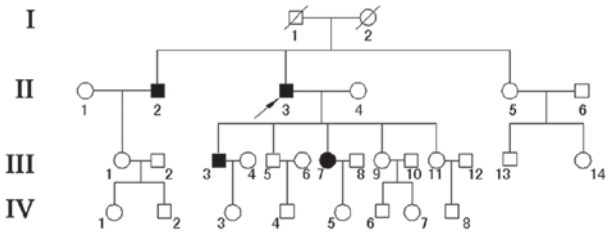


Figure 1. Pedigree chart of a family with Brugada syndrome. The affected family members are indicated by the filled symbols. The proband is indicated by an arrow (II3).

conservation of amino acids in $Na_v1.5$ protein was analyzed among the following species: Humans (*Homo sapiens*), orangutans (*Pongo abelii*), chickens (*Gallus gallus*), mice (*Mus musculus*), rats (*Rattus norvegicus*) and dogs (*Canis lupus familiaris*). ClustalW was used to align these protein sequences (http://www.ebi.ac.uk/Tools/msa/clustalw2/).

PCR-restriction fragment length polymorphism (RFLP) analysis. Mutation c.4282G>T (p.A1428S) disrupts an *Nsi*1 restriction site, which allowed us to perform PCR-RFLP analysis to confirm the mutation and test whether the mutation co-segregated with the disease in the family as described previously (24). Briefly, PCR amplification was performed on exon 24 containing the A1428S mutation of the *SCN5A* gene, following the aforementioned method. The 488-bp PCR product was digested with 10 units *Nsi*1 (New England Biolabs, Ipswich, MA, USA) at 37˚C overnight. The resulting digestion products were separated on 1.5% polyacrylamide gels and the DNA samples were separated by electrophoresis overnight at 150 V. The DNA bands were visualized by silver staining.

Cell cultures. Human embryonic kidney 293 (HEK293T) cells were purchased from the American Type Culture Collection (Manassas, VA, USA). These cells were cultured in Dulbecco's modified Eagle's medium (Sigma-Aldrich, St. Louis, MO, USA) containing 10% fetal bovine serum (Life Technologies, Paisley, UK), 2 mM L-glutamine, 100 U/ml penicillin G and 10 mg/ml streptomycin (Gibco-BRL, Burlington, ON, Canada) at 37˚C in a humidified atmosphere containing 5% CO_2. Cells were plated on poly-L-lysine-coated glass cover slips (12 mm) (Carl Zeiss, Inc., Oberkochen, Germany) and transiently transfected with wild-type (WT) *SCN5A*/pEGFP-N2 or mutation type (MT) *SCN5A*/pEGFP-N2 (2-5 μg) using Lipofectamine® 2000 (Invitrogen Life Technologies, Carlsbad, CA, USA) as previously described (20,25). Green fluorescent protein (GFP) was used as a marker to localize the protein within the cell. Cells expressing GFP, identified by green fluorescence, were selected for experiments, as shown in Fig. 2.

Electrophysiological recordings. Macroscopic sodium currents from the transfected cells were recorded at room temperature (21-24˚C) using the whole-cell patch clamp technique and an Axopatch 200B amplifier (Axon Instruments, Foster City, CA, USA). The extracellular solution contained: 70 mM NaCl, 80 mM CsCl, 5.4 mM KCl, 2 mM $CaCl_2$, 1 mM $MgCl_2$, 10 mM D-glucose and 10 mM HEPES (adjusted with CsOH to pH 7.3). The patch pipettes were

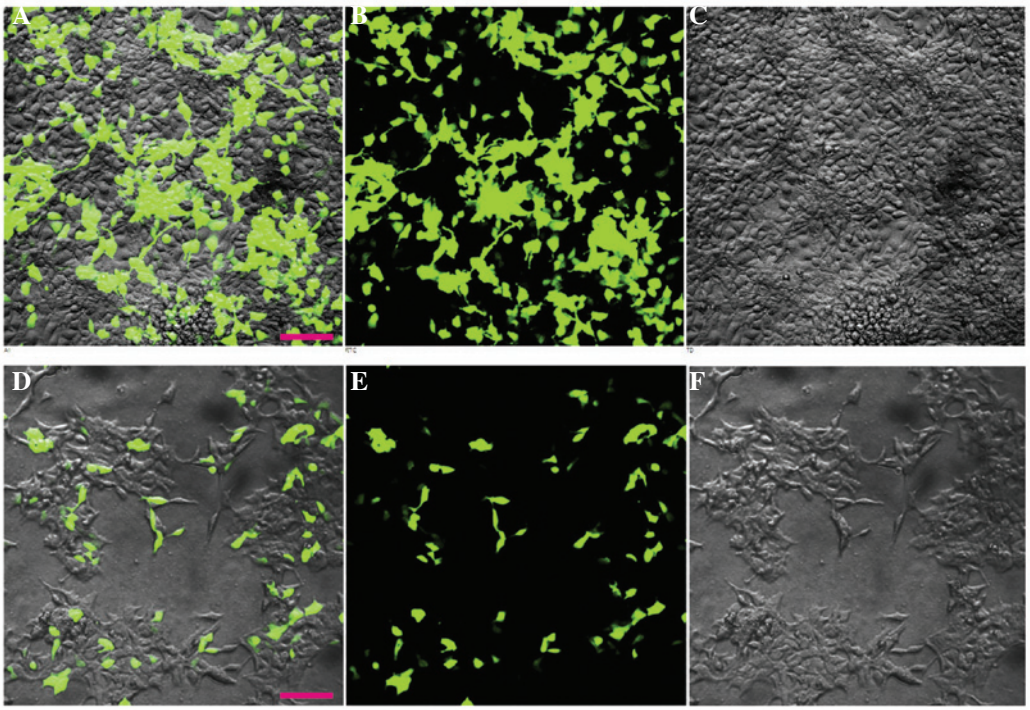


Figure 2. Representative bright-field and fluorescent images of HEK cells transfected with the *SCN5A* and *GFP* genes on a vector. HEK cells transfected with a vector containing the coding sequences of either wild-type (WT) or mutant (A1428S) Na^+ channels and green fluorescent protein (GFP) showed fluorescence, while the control HEK cells showed no fluorescence. Scale bar=50 μm. (A) Merge of bright-field and fluorescent images with GFP, (B) fluorescent images with GFP and (C) bright-field images of HEK293T cells transfected with a vector containing the coding of wild-type (WT) Na^+ channels. (D) Merge of bright-field and fluorescent images with GFP, (E) fluorescent images with GFP and (F) bright-field images of HEK293T cells transfected with a vector containing the coding of mutant (A1428S) Na^+ channels. For these images the cells were plated at a similar density 36 h prior to imaging. HEK, human embryonic kidney; GFP, green fluorescent protein.

fabricated from borosilicate glass capillaries (outer diameter, 1.5 mm; inner diameter, 1 mm; VitalSense Scientific Instruments, Wuhan, China) using a Sutter Model P-97 horizontal puller (Sutter Instrument Company, Novato, CA, USA). This typically had a resistance of 1-2 M when filled with the internal solution, which contained (in mM): 20 mM NaCl, 130 mM CsCl, 10 mM EGTA and 10 mM HEPES (adjusted to pH 7.2 with CsOH). Currents were amplified and filtered using an Axopatch 200B amplifier, and digitized with Digidata 1322A (Molecular Devices, Union City, CA, USA) at 5 kHz following analog filtering with the four-pole low-pass Bessel (2 kHz) of the amplifier. pCLAMP 9.0 and Origin 8.5 (OriginLab Corporation, Northampton, MA, USA) software were used for data acquisition and analysis, respectively. Series resistance compensation was used to improve the voltage-clamp control (70-80%). Peak current were normalized by the membrane capacitance and showed as the current density (pA/pF). Membrane conductance (G) was defined as $I/(V\text{-}E_{rev})$, where I was the peak amplitude, V was the test voltage and E_{rev} was the reversal potential of sodium currents. The steady-state inactivation curve was studied using a double-pulse protocol, in which the test voltage was stepped to -10 mV, 200 msec long, and preceded by 200 msec preconditioning pulses from -140 to -30 mV in 10-mV steps. The plots of voltage-dependent steady-state activation and inactivation were fitted by the Boltzmann equation: $1/[1+\exp(V\text{-}V_{1/2})/k]$, where $V_{1/2}$ was the voltage at which the sodium current was half-maximally activated, and k was the slope factor. Recovery from inactivation was examined by applying a 50-msec conditioning pulse to -20 mV from a holding potential of -120 mV, followed by a recovery interval of variable duration (2-10,000 msec) and a test pulse of -20 mV. The recovery time-course was fitted with the biexponential function: $I/I_{max} = A_o+A_f[1\text{-}\exp(-t/\tau_f)]+As[1\text{-}\exp(-t/\tau_s)]$, where τ and A were the time constants and the corresponding relative amplitudes, respectively.

Statistical analysis. Results are presented as the mean ± standard error of the mean with sample sizes (n) indicating the number of cells from which the data were obtained. Statistical significance was assessed using the Student's t-test. $P<0.05$ was considered to indicate a statistically significant difference.

Results

Pedigree and clinical features of the family. The proband, a 58-year-old patient (II3) was admitted to the emergency care unit due to syncope during walking with spontaneous recovery. A 12-lead ECG was performed without a drug challenge test and showed ST-segment elevation in the right precordial leads (Fig. 3). In V2 and V3, the QRS complex showed a typical BrS 1 pattern with a coved-shape ST-segment. The history of the patient revealed that he had one episode of syncope in the past, and his familial history revealed that two children (III3 and III7) and one brother (II2) had experienced several episodes of dizziness and syncope. Subsequent to a certain dose of flecainide challenge, all of the affected individuals showed right bundle branch block and coved-type ST-segment

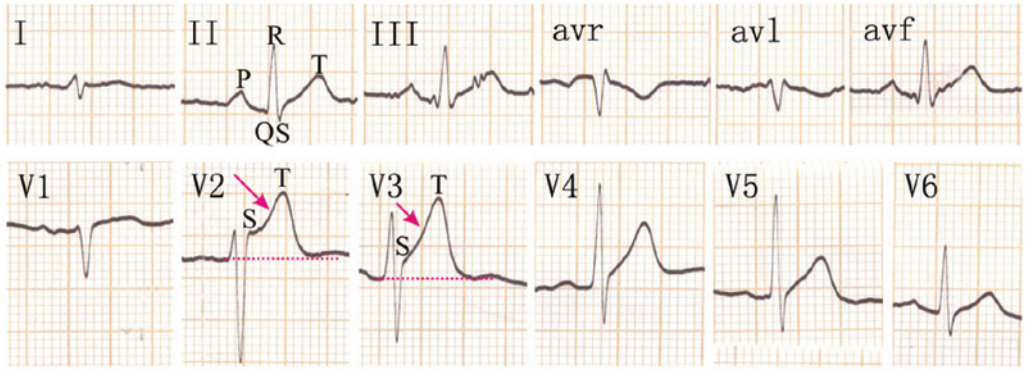


Figure 3. Diagnostic BrS ECG. Twelve-lead electrocardiogram showing a representative type 1 BrS ECG with coved ST-segment elevation in the right precordial leads, particularly in V2 and V3. The arrows indicate the coved ST-segment elevation. BrS, Brugada syndrome; ECG, electrocardiography.

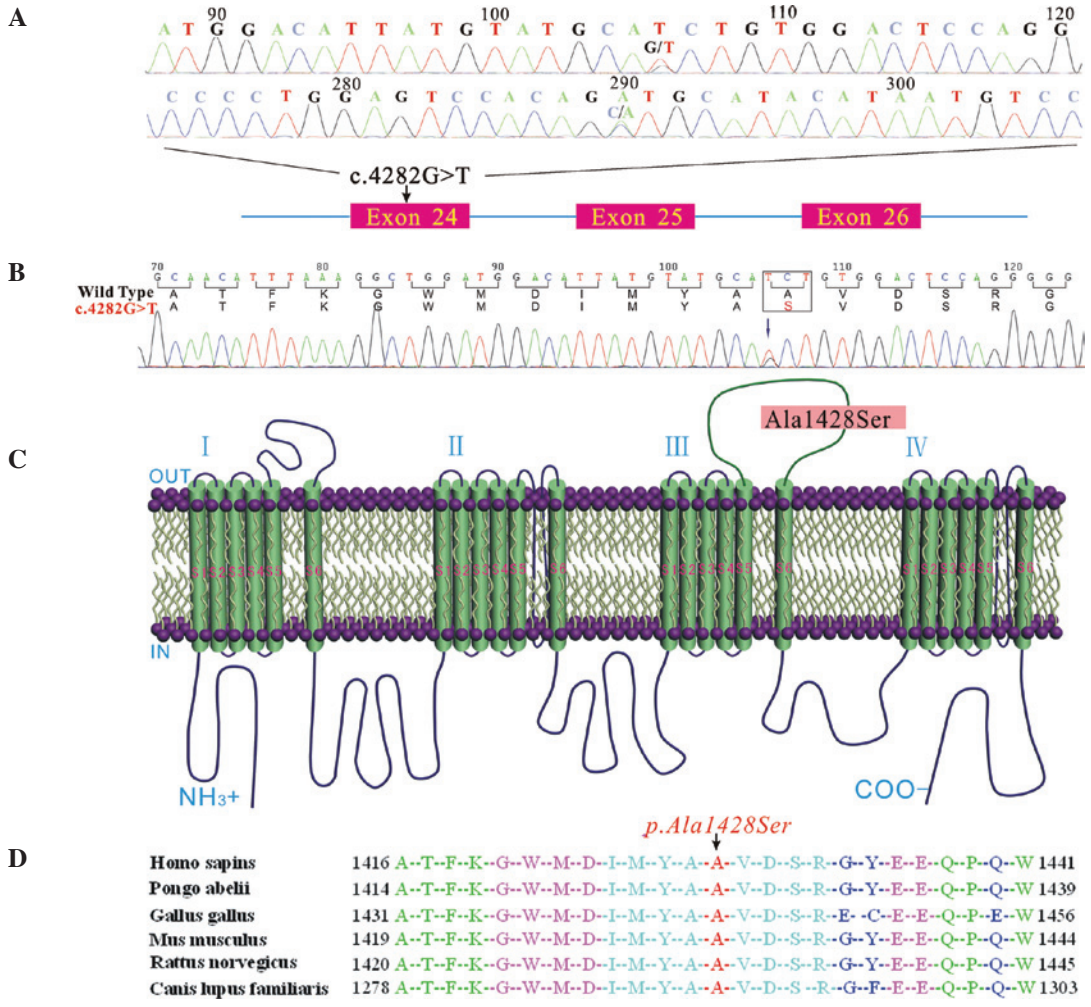


Figure 4. Analysis the mutation of the *SCN5A* gene in the studied family and changes in the $Na_v1.5$ channel α subunit protein sequences following mutation. (A) Sequencing chromatograms of the proband from the family showing a novel missense mutation c.4282G>T in the *SCN5A* gene in exon 24. (B) c.4282G>T results in a heterozygous p.A1428S mutation, which is located in the (C) DIII-S5/S6 of the $Na_v1.5$ channel α subunit protein. (D) ClustalW alignment of the $Na_v1.5$ channel α subunit protein shows that the alanine residue at position 1,428 is highly conserved across humans (*Homo sapiens*), orangutans (*Pongo abelii*), chickens (*Gallus gallus*), mice (*Mus musculus*), rats (*Rattus norvegicus*) and dogs (*Canis lupus familiaris*).

elevation. However, none of the clinical features of the proband were identified in the other members of his family.

Genetic analysis. To identify the molecular basis of BrS in the proband, exons 1-28 of the dystrophin gene were amplified by PCR. By direct bidirectional sequencing of the PCR products in the proband, a heterozygous missense single nucleotide at position 4,282 (c.4282G>T) in exon 24 of the *SCN5A* gene was revealed (Fig. 4A); this was confirmed by repeating the experiment. The missense nucleotide resulted in



Figure 5. PCR-restriction fragment length polymorphism analysis of the mutation in exon 24 of the *SCN5A* gene. The c.4282G>T mutation resulted in the appearance of an *Nsi*1 restriction site. The mutation-type PCR product was cut by *Nsi*1, yielding two shorter DNA fragments of 329 and 159 bp. All affected individuals in the family were heterozygous for the p.A1428S mutation (three fragments: 488, 329 and 159 bp; II2, II3, III3 and III7). However, the wild-type PCR product could not be cut by *Nsi*1, resulting in only one DNA fragment of 488 bp. The PCR products were shown by electrophoresis in a 1.5% agarose gel stained with ethidium bromide. PCR, polymerase chain reaction.

an amino acid change from alanine to serine at position 1,428 (abbreviated as p.A1428S, Fig. 4B) in the DIII-S5/S6 of the $Na_v1.5$ channel (Fig. 4C). Ala1428 is highly conserved among humans (*Homo sapiens*), orangutans (*Pongo abelii*), chickens (*Gallus gallus*), mice (*Mus musculus*), rats (*Rattus norvegicus*) and dogs (*Canis lupus familiaris*) (Fig. 4D).

RFLP analysis. Mutation c.4282G>T (p.A1428S) disrupts an *Nsi*1 restriction site. To confirm the mutation and test whether the mutation co-segregated with the disease in the family, the novel variation detected in exon 24 of the *SCN5A* gene was further evaluated in the other available family members, as well as in the normal control subjects using RFLP analysis. The PCR fragment containing mutation Ala1428Ser was able to be cut by the enzyme; therefore, the RFLP results revealed the presence of the MT (329 and 159-bp bands) and WT (488-bp bands) alleles (II2, III3, III7 and proband II3, Fig. 5). However, the DNA samples from the 100 normal males and the other unaffected family members were also analyzed by RFLP, and the results revealed that the unaffected members of the family and the 100 normal controls only had the WT allele (488-bp bands) (Fig. 5). These results further suggest that this novel mutation (c.4282G>T, p.A1428S) of the *SCN5A* gene is not a rare polymorphism, but a causative mutation for BrS in the proband.

Biophysical properties of the A1428S mutant. To understand the clinical phenotypes of this patient, the biophysical properties of the WT and MT channels were studied. The WT $Na_v1.5$ channels and channels expressed from the mutated cDNAs of *SCN5A* were studied in transfected HEK293 cells. Cells expressing GFP, identified by green fluorescence (Fig. 2), were selected for whole-cell patch clamp recordings. The HEK293 cells themselves did not exhibit a substantial level of I_{Na}. By contrast, cells transfected with the WT *SCN5A* cDNA had a large I_{Na} (Fig. 6A). A marked reduction in current amplitudes was observed with the mutation A1428S (Fig. 6B). Fig. 6C shows the V_m dependence of the averaged current density. The A1428S mutation did not change the shape of I-V curve, but significantly reduced the peak current density without altering the reversal potential and the voltage dependence of the I_{Na} peak. At -30 mV, the mean peak sodium current density was reduced from -220.82 pA/pF (WT) to -136.44 pA/pF (A1428S) (Fig. 6D, $P<0.05$). The non-significant variation of the reversal potentials of WT (30.9±1.2 mV, n=10) and A1428S (29.8±2.4 mV, n=10) indicated that the mutations had no impact on channel selectivity, as was also evidenced by the I-V curves (Fig. 6C).

The effects of the A1428S mutation on the V_m dependence of channel activation are shown in Fig. 6E. The normalized conductance-V_m association was constructed and it was revealed that the V_m-dependent activation was the same in the WT channel ($V_{1/2}$, -43.86±1.39 mV; k, 5.91±0.76 mV) and the A1428S mutant ($V_{1/2}$, -41.63±1.36 mV; k, 6.10±0.69 mV). To compare the inactivation kinetics of the WT and A1428S mutant, whole-cell currents at various potentials were fitted to a biexponential function. As shown in Fig. 6F, the steady-state inactivation was not significantly different between the WT channel ($V_{1/2}$, -91.50±1.14 mV; k, 7.01±0.48 mV) and the A1428S mutant ($V_{1/2}$, -92.33±1.39 mV; k, 7.51±0.73 mV). Recovery from the inactivation of the WT channel and the A1428S mutant was then assessed using a double-pulse protocol, as shown in Fig. 6G. The biexponential fit to recovery curve showed no significant difference between the WT channel (τ_f, 5.58±1.36 sec; τ_s, 40.06±21.32 sec), and the A1428S mutant (τ_f, 6.07±1.27 sec; τ_s, 23.08±6.48 sec) ($P>0.05$).

Discussion

In this study, a novel heterozygous mutation c.4282G>T in the *SCN5A* gene that caused BrS was presented. It was shown that the mutation caused a significant reduction in Na^+ current, suggesting its involvement in the pathogenesis of the arrhythmic phenotype seen in the studied family. Diagnosis of BrS in the proband was based on the ECG, which showed a coved-type ST-segment elevation in the right precordial leads, particularly in V2 and V3 (Fig. 3). To identify the disease-causing gene in the proband, all coding regions (exons 1-28) of the *SCN5A* gene were PCR-amplified and sequenced with DNA. A novel missense mutation (c.4282G>T) in exon 24 of the *SCN5A* gene was identified, which resulted in an amino acid change from alanine to serine at position 1,428 in the DIII-S5/S6 of the $Na_v1.5$ channel (Fig. 4). This mutation was further confirmed by PCR-RFLP analysis, which showed that the PCR fragment containing mutation A1428S could be cut by the *Nsi*1 restriction enzyme, yielding two shorter DNA fragments of 329 and 159 bp. These fragments were not present in individuals with the WT allele (Fig. 5). These results suggested the *SCN5A* mutation led to the dysfunction of the $Na_v1.5$ channel, which caused an episode of sudden collapse during walking.

It is well known that the *SCN5A* gene encodes the α subunit of the human cardiac $Na_v1.5$ channel, which is a transmembrane protein composed of the main pore-forming α-subunit and two subsidiary β-subunits (β_1 and β_2) (26,27). There is considerable evidence that $Na_v1.5$ forms a section of a macromolecular complex (28) and that its function is modulated by cytoskeletal proteins, including tubulin (29), syntrophin and dystrophin (30). Considering these interactions between $Na_v1.5$ and the cytoskeletal proteins, it is conceivable that abnormal $Na_v1.5$ proteins affect the function of the cytoskeleton and the structural integrity of cardiomyocytes. A report recently showed that patients with BrS with a *SCN5A* mutation exhibit enlarged right and left ventricles compared with individuals without an *SCN5A* mutation (31). Furthermore, the $Na_v1.5$ channel plays a key role in cardiac excitability

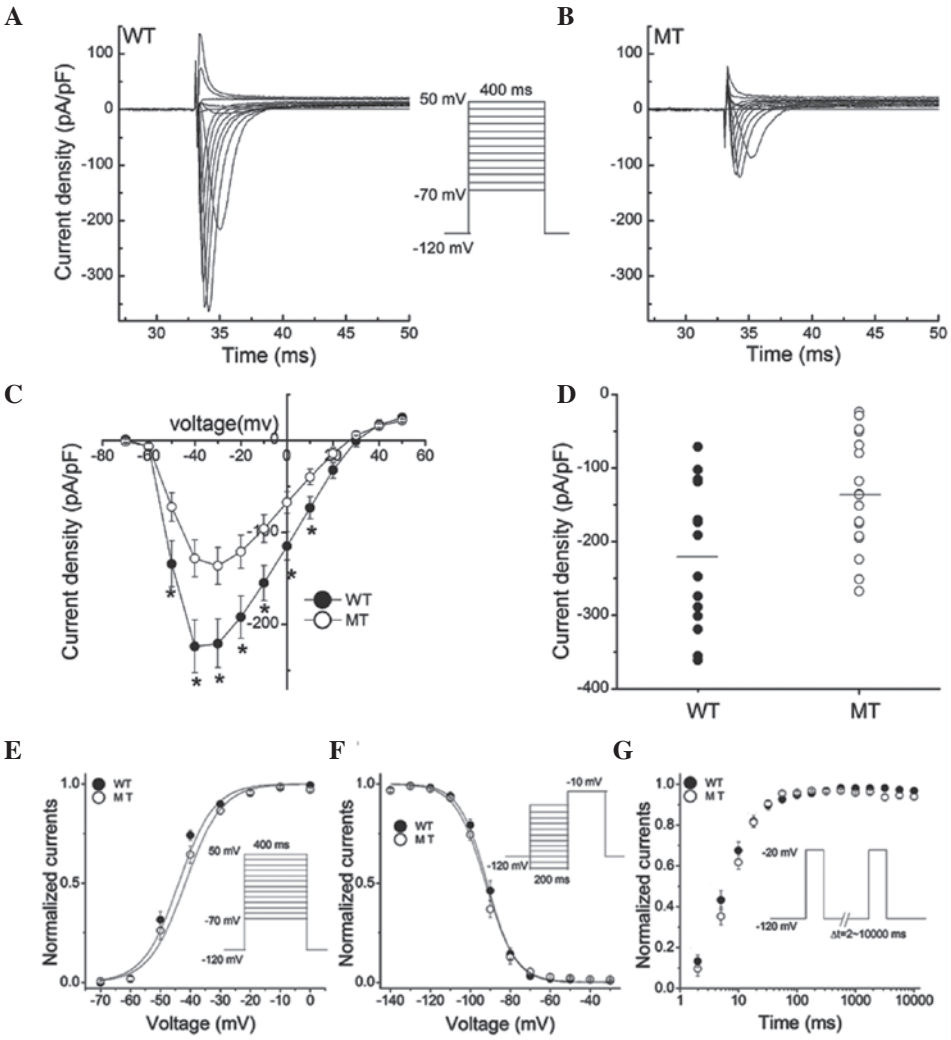


Figure 6. Properties of sodium current recorded from HEK293T cells transfected with *SCN5A* WT or p.A1428S channels. (A and B) Representative current traces of HEK293T cells transfected with (A) *SCN5A* WT and (B) p.A1428S channel. (C) Current-voltage (I-V) association of WT (n=14) and p.A1428S channel (n=16). (D) Mean peak sodium current density recorded at -30 mV. The difference in the current densities between the WT (n=14) and p.A1428S channels (n=16) was statistically significant. (E and F) Kinetics of sodium channel activation and inactivation: (E) Voltage-dependant steady-state activation (n=13) and (F) inactivation (n=16). (G) Recovery from inactivation was assessed for the WT and MT (n=10) utilizing a two-pulse protocol. HEK, human embryonic kidney; WT, wild-type; MT, mutation-type.

and conduction. It is responsible for the rapid upstroke of the action potential (AP) caused by the rapid entry of Na^+ ions into cardiac myocytes. In the present study, electrophysiological characterization of the $Na_v1.5$ mutation, A1428S, revealed that Na^+ current density was significantly decreased compared with that in the WT, which affected the AP of cardiomyocytes. Therefore, dysfunctions of this channel can cause BrS.

The $Na_v1.5$ channel α subunit consists of four homologous domains, and each domain contains six α-helical transmembrane repeats. In the present study, the substituted amino acid p.A1428S was located at the fifth α-helical transmembrane segment of domain III-S5/S6. Mutations located at this region have been previously reported, including N1380K (32), although few have been characterized by functional studies. The present findings indicate that neither the steady-state activation or inactivation, nor the recovery from inactivation differs between the A1428S mutation and the WT. These results revealed that the DIII-S5/S6 of the $Na_v1.5$ channel α subunit was not involved in regulating the recovery from inactivation, or steady-state activation or inactivation. This result was consistent with the previous functional studies reporting that the carboxyl-terminal of the cardiac sodium channel may play an important role in controlling the gate property of the channel (33,34). Rivolta *et al* (35) reported that the mutation Y1795H, which contributes to BrS, affected steady-state and fast inactivation, as well as current density. Similar findings were also observed in the BrS-causing C1859S mutation, as reported by Petitprez *et al* (36). Additionally, change of steady-state activation was observed in the T1620M and S1710L mutations (37). These results demonstrated that the carboxyl-terminal of the cardiac sodium channel plays a critical role in the regulation of the gating property of the channel. No change in the gating property of the channel was observed in the A1428S mutation in the present study.

In conclusion, to the best of our knowledge, this is the first description of a novel heterozygous missense mutation, A1428S, in exon 24 of the *SCN5A* gene in a family with BrS. This finding expands the mutation spectrum of the *SCN5A* gene and may prove useful and valuable for genetic counseling and

prenatal diagnosis in families with BrS. Electrophysiological characterization of the $Na_v1.5$ mutation, A1428S, revealed that the fifth α-helical transmembrane segment of DIII-S5/S6 did not regulate the recovery from inactivation, or steady-state activation or inactivation. However, the decreased $Na_v1.5$ activity caused by the A1428S mutation supports the hypothesis that a reduction in $Na_v1.5$ function is involved in the pathogenesis of BrS. This structural-functional study of the $Na_v1.5$ channel enhances the current understanding of the pathophysiological function of the channel and provides potential preventive and therapeutic approaches to heart disease.

Acknowledgements

This study was supported by grants from the National Natural Science Foundation of China (nos. 31301024 and 81400462) and the Natural Science Foundation of Hubei Province of China (no. 2012FKB02441).

References

1. Moreau A, Keller DI, Huang H, *et al*: Mexiletine differentially restores the trafficking defects caused by two brugada syndrome mutations. Front Pharmacol 3: 62, 2012.
2. Brugada P and Brugada J: Right bundle branch block, persistent ST segment elevation and sudden cardiac death: a distinct clinical and electrocardiographic syndrome. A multicenter report. J Am Coll Cardiol 20: 1391-1396, 1992.
3. Bhar-Amato J, Nunn L and Lambiase P: A review of the mechanisms of ventricular arrhythmia in brugada syndrome. Indian Pacing Electrophysiol J 10: 410-425, 2010.
4. Vohra J: Diagnosis and management of Brugada Syndrome. Heart Lung Circ 20: 751-756, 2011.
5. Wilde AA, Antzelevitch C, Borggrefe M, *et al*: Proposed diagnostic criteria for the Brugada syndrome: consensus report. Circulation 106: 2514-2519, 2002.
6. Antzelevitch C, Brugada P, Borggrefe M, *et al*: Brugada syndrome: report of the second consensus conference. Heart Rhythm 2: 429-440, 2005.
7. Chen Q, Kirsch GE, Zhang D, *et al*: Genetic basis and molecular mechanism for idiopathic ventricular fibrillation. Nature 392: 293-296, 1998.
8. Antzelevitch C, Pollevick GD, Cordeiro JM, *et al*: Loss-of-function mutations in the cardiac calcium channel underlie a new clinical entity characterized by ST-segment elevation, short QT intervals, and sudden cardiac death. Circulation 115: 442-449, 2007.
9. Burashnikov E, Pfeiffer R, Barajas-Martinez H, *et al*: Mutations in the cardiac L-type calcium channel associated with inherited J-wave syndromes and sudden cardiac death. Heart Rhythm 7: 1872-1882, 2010.
10. Watanabe H, Koopmann TT, Le Scouarnec S, *et al*: Sodium channel β1 subunit mutations associated with Brugada syndrome and cardiac conduction disease in humans. J Clin Invest 118: 2260-2268, 2008.
11. Hu D, Barajas-Martínez H, Medeiros-Domingo A, *et al*: A novel rare variant in SCN1Bb linked to Brugada syndrome and SIDS by combined modulation of Na(v)1.5 and K(v)4.3 channel currents. Heart Rhythm 9: 760-769, 2012.
12. Hu D, Barajas-Martinez H, Burashnikov E, *et al*: A mutation in the beta 3 subunit of the cardiac sodium channel associated with Brugada ECG phenotype. Circ Cardiovasc Genet 2: 270-278, 2009.
13. Kattygnarath D, Maugenre S, Neyroud N, *et al*: MOG1: a new susceptibility gene for Brugada syndrome. Circ Cardiovasc Genet 4: 261-268, 2011.
14. Delpón E, Cordeiro JM, Núñez L, *et al*: Functional effects of KCNE3 mutation and its role in the development of Brugada syndrome. Circ Arrhythm Electrophysiol 1: 209-218, 2008.
15. Giudicessi JR, Ye D, Tester DJ, *et al*: Transient outward current (I(to)) gain-of-function mutations in the KCND3-encoded Kv4.3 potassium channel and Brugada syndrome. Heart Rhythm 8: 1024-1032, 2011.
16. Medeiros-Domingo A, Tan BH, Crotti L, *et al*: Gain-of-function mutation S422L in the KCNJ8-encoded cardiac K(ATP) channel Kir6.1 as a pathogenic substrate for J-wave syndromes. Heart Rhythm 7: 1466-1471, 2010.
17. Ueda K, Hirano Y, Higashiuesato Y, *et al*: Role of HCN4 channel in preventing ventricular arrhythmia. J Hum Genet 54: 115-121, 2009.
18. Schulze-Bahr E, Eckardt L, Breithardt G, *et al*: Sodium channel gene (SCN5A) mutations in 44 index patients with Brugada syndrome: different incidences in familial and sporadic disease. Hum Mutat 21: 651-652, 2003.
19. Priori SG, Napolitano C, Gasparini M, *et al*: Clinical and genetic heterogeneity of right bundle branch block and ST-segment elevation syndrome: A prospective evaluation of 52 families. Circulation 102: 2509-2515, 2000.
20. Priori SG, Napolitano C, Gasparini M, *et al*: Natural history of Brugada syndrome: insights for risk stratification and management. Circulation 105: 1342-1347, 2002.
21. Cai F, Zhu J, Chen W, *et al*: A novel PAX6 mutation in a large Chinese family with aniridia and congenital cataract. Mol Vis 16: 1141-1145, 2010.
22. Zhu JF, Liu HH, Zhou T and Tian L: Novel mutation in exon 56 of the dystrophin gene in a child with Duchenne muscular dystrophy. Int J Mol Med 32: 1166-1170, 2013.
23. Wang Q, Li Z, Shen J and Keating MT: Genomic organization of the human SCN5A gene encoding the cardiac sodium channel. Genomics 34: 9-16, 1996.
24. Wang Q, Liu M, Xu C, *et al*: Novel CACNA1S mutation causes autosomal dominant hypokalemic periodic paralysis in a Chinese family. J Mol Med (Berl) 83: 203-208, 2005.
25. Tfelt-Hansen J, Winkel BG, Grunnet M and Jespersen T: Inherited cardiac diseases caused by mutations in the Nav1.5 sodium channel. J Cardiovasc Electrophysiol 21: 107-115, 2010.
26. Adsit GS, Vaidyanathan R, Galler CM, *et al*: Channelopathies from mutations in the cardiac sodium channel protein complex. J Mol Cell Cardiol 61: 34-43, 2013.
27. Amin AS, Asghari-Roodsari A and Tan HL: Cardiac sodium channelopathies. Pflugers Arch 460: 223-237, 2010.
28. Shy D, Gillet L and Abriel H: Cardiac sodium channel NaV1.5 distribution in myocytes via interacting proteins: the multiple pool model. Biochim Biophys Acta 1833: 886-894, 2013.
29. Casini S, Tan HL, Demirayak I, *et al*: Tubulin polymerization modifies cardiac sodium channel expression and gating. Cardiovasc Res 85: 691-700, 2010.
30. Gavillet B, Rougier JS, Domenighetti AA, *et al*: Cardiac sodium channel Nav1.5 is regulated by a multiprotein complex composed of syntrophins and dystrophin. Circ Res 99: 407-414, 2006.
31. van Hoorn F, Campian ME, Spijkerboer A, *et al*: SCN5A mutations in Brugada syndrome are associated with increased cardiac dimensions and reduced contractility. PLoS One 7: e42037, 2012.
32. Crotti L, Marcou CA, Tester DJ, *et al*: Spectrum and prevalence of mutations involving BrS1-through BrS12-susceptibility genes in a cohort of unrelated patients referred for Brugada syndrome genetic testing; implications for genetic testing. J Am Coll Cardiol 60: 1410-1418, 2012.
33. Motoike HK, Liu H, Glaaser IW, *et al*: The Na^+ channel inactivation gate is a molecular complex: a novel role of the COOH-terminal domain. J Gen Physiol 123: 155-165, 2004.
34. Kass RS: Sodium channel inactivation in heart: a novel role of the carboxy-terminal domain. J Cardiovasc Electrophysiol 17 Suppl 1: S21-S25, 2006.
35. Rivolta I, Abriel H, Tateyama M, *et al*: Inherited Brugada and long QT-3 syndrome mutations of a single residue of the cardiac sodium channel confer distinct channel and clinical phenotypes. J Biol Chem 276: 30623-30630, 2001.
36. Petitprez S, Jespersen T, Pruvot E, *et al*: Analyses of a novel SCN5A mutation (C1850S): conduction vs. repolarization disorder hypotheses in the Brugada syndrome. Cardiovasc Res 78: 494-504, 2008.
37. Shirai N, Makita N, Sasaki K, *et al*: A mutant cardiac sodium channel with multiple biophysical defects associated with overlapping clinical features of Brugada syndrome and cardiac conduction disease. Cardiovasc Res 53: 348-354, 2002.